УДК 538.9
doi: 10.18101/ 978-5-9793-0898-2-111-120

STUDY OF ANTICANCER DRUG RELEASE FROM NANOPARTICLES BY RAMAN SPECTROSCOPY

© ***Erdene-Ochir G***, Department of Chemistry,
Soongsil University
Seoul, Korea,
Department of Physics, National University of Mongolia
Ulaanbaatar, Mongolia
E-mail: erdeneochir_g@num.edu.mn

© ***Joo S.-W.***, Department of Physics,
National University of Mongolia
Ulaanbaatar, Mongolia
E-mail: erdeneochir_g@num.edu.mn

Drug-conjugated gold nanoparticles (AuNPs) system was prepared by self-assembly. We monitored the intracellular release of drug molecules from AuNPs inside the single cell using dark-field microscopy-combined Raman spectrometer by means of label-free real-time measurements. Imatinib (IMT) and topotecan (TOPO) which form weak covalent bonds with AuNPs were found to detach easily due to intracellular glutathione (GSH) whereas 4-carboxyl benzenethiol used as cross-linker remains on the surface of AuNPs.
Keywords: surface-enhanced Raman scattering, gold nanoparticles, drug delivery, dark-field microscopy.

Introduction

Nanomaterials have been received great interest from researchers in a variety of bionanotechnological area such as targeted drug delivery, cellular imaging and anticancer therapies for past decades. Particularly, gold nanoparticles (AuNPs) play an important role due to their facile synthesize, biocompatibility and low cytotoxicity. It is now well known that AuNPs are good substrate to enhance originally weak Raman scattering signals.

Fluorescence microscopy is widely utilized to monitor the release of a drug molecules from nano-sized carriers. But very few numbers of drugs give a fluorescence. So it requires to tag non-fluorescent molecules to monitor by fluorescence microscopy. Here we show that Raman spec-

trometer can be used to monitor intracellular drug release from AuNPs at the single cell level.

Experimental section

Sample preparation. Negatively charged AuNPs were synthesized using the citrate reduction method. 30 ml of 1.4 mM $HAuCl_4$ solution was boiled and vigorously stirred on the hot plate. When it is boiled, 3 ml of 55 mM sodium citrate solution was added quickly, and boiling was continued for 1h.

The final concentrations of topotecan (TOPO, ~2×10^{-5} M) and imatinib (IMT, ~10^{-5} M) can be fabricated on AuNPs via self-assembly for 12 h. One of the most versatile methods of bioconjugation may be achieved using 1-ethyl-3-[3-dimethylaminopropyl] carbodiimide hydrochloride (EDC), which is an amine-reactive cross-linker.[17] In a typical DFM/Raman experiments, 1 ml of each of TOPO (1 mM) and IMT (1 mM) in distilled water were subsequently added to 100 ml of aqueous AuNPs solution. This was followed by the addition of 1 ml of 4-carboxylic benzenethiol (CBT) which is used as a linker for conjugating transferrin (Tf, minimum ≥98%)–EDC. After 15 min, the prepared sample was mixed with a 500 ml of a 1:1 mixture of Tf (~10^{-5} M) and EDC (~10^{-5} M) and was left for overnight. The conjugate was centrifuged at a 4000 g for 5 min and redispersed in 100 ml of distilled water.

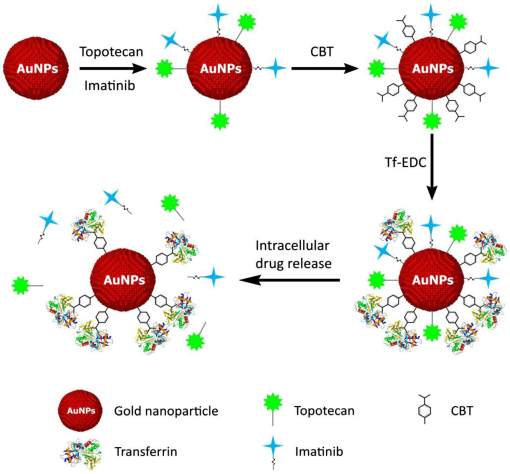

Fig. 1. Schematic diagrams of the conjugation of the two anticancer drugs of IMT and TOPO on AuNPs with the targeting Tf protein via the CBT linker. Raman spectroscopy was used to observe the combinatory drug release from the conjugate

Figure 2(a) shows the IR spectra of Tf assembled on AuNPs in the wavenumber region between 800 and 3800 cm^{-1}. It was found that IMT was assembled on AuNPs. The vibrational feature changes including several additional bands indicate the formation of the amide linkage as a result of the coupling reaction between the COOH group of CBT assembled on Au surfaces and the amine group of Tf.

We performed an SERS study to confirm the coupling reaction as illustrated in Fig. 2(b). The strong bands found at 992, 1029, 1298, and 1585 cm^{-1} could be ascribed to those of aromatic rings (pyridine ring, aminopyrimidine ring, methylbenzene ring, benzamide ring, and N-methylpiperazine ring of IMT).[27] Upon conjugation with Tf onto CBT-coated AuNPs, we observed several vibrational modes ascribed to CBT including the two major aromatic ring bands at 1589 and 1076 cm^{-1} among several spectral features. We also found that the ν(SH) band at ~2560 cm^{-1} of CBT disappeared upon adsorption on AuNPs. Consulting the earlier vibrational assignments,[26–28] we analyzed the Raman spectrum of CBT and the two drugs. The Raman spectrum of TOPO on AuNPs can be ascribed to those of the aromatic ring modes of a camptothecin compound.[16]

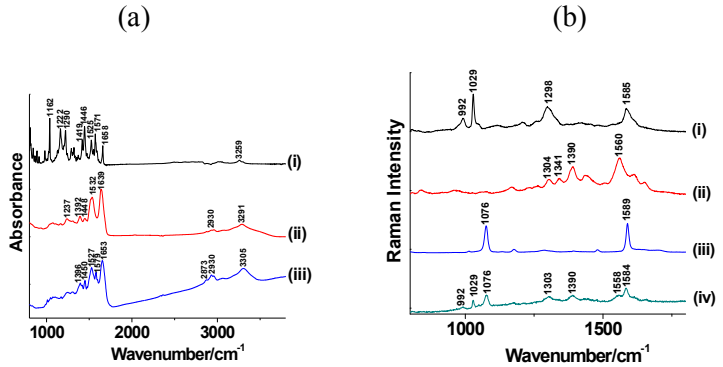

Fig. 2. (a) ATR spectra of solid (i) IMT and (ii) Tf. (iii) Infrared spectra of AuNP–IMT/TOPO–CBT–Tf in the wavenumber region between 800 and 3800 cm^{-1}. The infrared TOPO spectrum[16] was omitted due to the weakness in comparison with the other IMT and Tf bands. (b) Raman spectra of (i) IMT and (ii) TOPO on AuNPs. SERS spectra of (iii) CBT and (iv) of AuNP–IMT/TOPO–CBT–Tf in the wavenumber region between 800 and 1800 cm^{-1}

Figure 3(a) and (b) shows the SERS spectra of IMT on AuNPs after treatment with 2 mM GSH. However, the data is not included here, it was found that IMT appeared to be undetached in cell culture media but was released after treatment with GSH. Figure 3 (c) shows release of IMT from AuNPs by GSH (2 mM) with 90 min for the CBT linkers. It was found that the SERS peaks of drugs became much weaker with respect to those of the CBT linker. As shown in Fig. 3(c), not CBT but TOPO/IMT peak intensities decreased to suggest that this change should be due to the desorption instead of the aggregation conditions. Our independent dynamic light scattering measurements showed that the particle diameters did not change significantly after treating 2 mM GSH for 60 min to support that the decrease in the SERS intensities is not directly related to the change in particle aggregation. All these results indicate that intracellular release of IMT can occur via GSH.

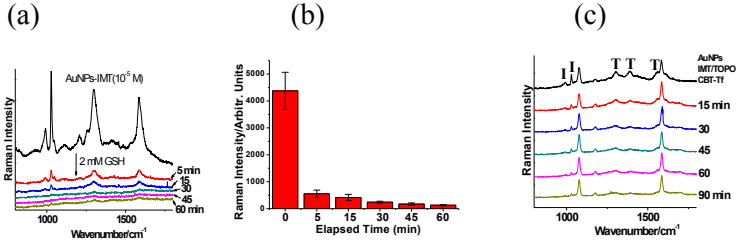

Fig. 3. (a) Release of IMT from AuNPs by GSH (2 mM) with an hour. The decrease in the SERS intensities of IMT indicated the desorption of IMT on AuNPs via GSH. Similar tests were performed for TOPO.[16] (b) Plot of the relative intensity ratios of the IMT band at 1030 cm_1 after treating GSH (2 mM) for 0–60 min. (c) SERS spectra of AuNP–IMT/TOPO–CBT–Tf after treating with GSH. 'I' and 'T' stand for IMT and TOPO peaks, respectively

Figure 4 shows the DFM images and corresponding SERS spectra at a certain local point inside a single K562 cell after the uptake of the CBT-modified AuNPs. The internalization of NPs was confirmed by z-depth-dependent SERS combined with DFM. The SERS spectra appeared to be consistent with the previous report.[22,28] We managed to find the Raman spectra for specific spots that contained the signatures of the vibrational bands of CBT, which indicates the presence of AuNPs at the locations. As shown in Fig. 4 (b), we could observe not any drug peaks but the CBT peaks from the AuNP–TOPO/IMT–CBT–Tf sample. This may be due to the drug release from AuNPs via intracellular GSH

as suggested from Fig. 3. As shown in Fig. 4, some of CBT-coated AuNPs were found to be taken up into intracellular compartments. Guided by the DFM images, we could localize the positions of AuNPs and checked the Raman spectra in a much more rapid way. For the SERS spectra pointed by the arrow, we did find quite prominent features of Tf-conjugated CBT peaks, which is evidence of presence of AuNPs at the positions. The arrow indicates the location of the AuNPs as determined according to the SERS spectra. DFM live cell imaging data indicated that the anticancer drug–AuNP conjugates entered into the K562 cell within 1 h. It was found that at least a part of TOPO was released from AuNPs via an intracellular GSH in the previous report.[16] This result may explain why we could not observe any strong drug peaks in the DFM and Raman images as shown in Fig. 4 after 24 h. It has to be mentioned that the cytosol solution caused significant decrease in SERS intensities. This result suggests that the attached drugs on AuNPs could be detached easily by intracellular contents after their endocytosis.

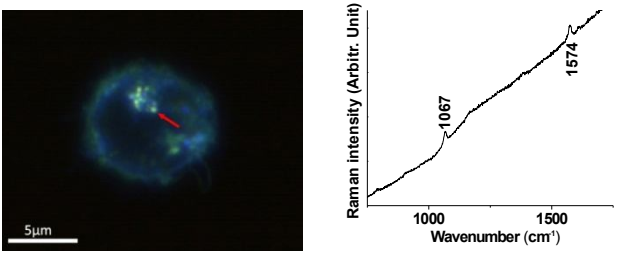

Fig. 4. DFM and SERS spectra of AuNP–IMT/TOPO–CBT–Tf embedded in a K562 cell. The arrows indicates the location of the AuNPs as determined according to the SERS spectra. The CBT-coated AuNPs were found to locate approximately a few mm inside the cell surfaces at the spot pointed by the arrows. Only the strongest Raman spectrum was presented, from the z-depth SERS spectra obtained to check the intracellular location

We also performed the experiments to monitor intracellular drug release of another anti-cancer drug, mitoxantrone (MTX), from the surface of AuNPs carriers by means of real-time label-free bimodal imaging with confocal Raman and fluorescence spectroscopy. The amount of MTX released was estimated by both the decrease in the surface-enhanced re-

sonance Raman scattering (SERRS) signal and the increase in the fluorescence intensity. MTX on AuNPs appeared to exhibit strong Raman intensities upon excitation at 633 nm through a resonance-enhancement process.[23,24] The detached MTX drug can be monitored by both a SERRS signal decrease and a fluorescence intensity increase upon irradiation. The signal decay profiles of the drug release from AuNPs appeared to be dissimilar for fluorescence quenching with SERRS and NSET.

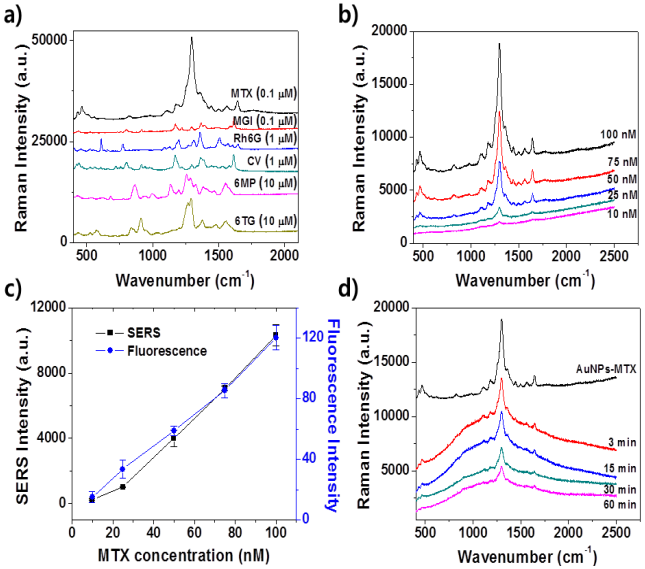

Fig. 5. (a)Comparative SERS spectra of MTX (0.1 μM) with malachite green (MGI, 0.1 μM), rhodamine 6G (Rh6G, 1 μM), crystal violet (CV, 1 μM), 6-mercaptopurine (6MP, 10 μM), and 6-thioguanine (6TG, 10 μM). (b) Concentration-dependent SERS spectra of MTX between 10–100 nM. (c) Quantitative aspects of SERS and fluorescence intensities as a function of the MTX concentration. Peaks at 1291 cm^{-1} were used to compare the relative intensities. Error bars demonstrate the standard deviation of three measurements. (d)GSH concentration-dependent SERS intensities of MTX (100 nM) on AuNP surfaces in an aqueous solution, exhibiting the background changes due to the increase in fluorescence

Fig. 6 shows the in vitro release of MTX from AuNPs in HeLa cells over a time interval of 0–120 min. We observed the AuNPs inside the cell membrane using a z-dependent SERRS method. Raman monitoring

implies that the SERRS intensities of MTX were decreased inside the cells in an hour. The decay profiles could be divided into two distinct regions as shown in Fig. 6c. In the first 45 min, a rather fast decay rate k of 0.0252 min^{-1} with a short half-life $t_{1/2}$ of 27.5 min was observed, whereas the rate became significantly slower, 0.0093 min^{-1} with a longer half-life of 101.4 min, after 45 min. The initial fast decay may be due to a bond breaking process between MTX and the AuNPs. The subsequent slower rate may be interpreted as the non-quantitative nature of the SERRS intensity such as hot spots, where only a few percent of the adsorbates can yield a majority of the total intensity.

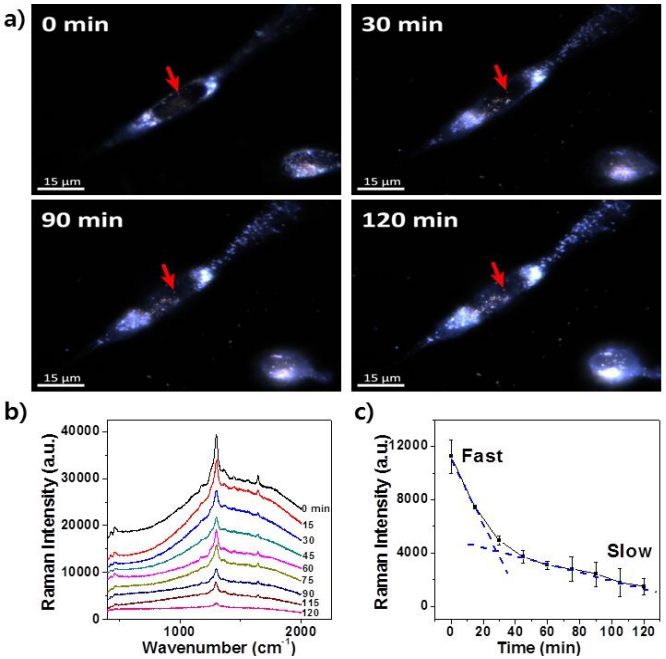

Fig. 6. (a) Photographs of the time-dependent in vitro dark-field microscopy (DFM) of live cell images. The arrows indicate the location of the AuNPs according to the SERS spectra. (b) Time-dependent SERRS spectra of MTX-conjugated AuNPs exhibiting the release of MTX. (c) Intensity of the SERRS spectra of MTX-AuNPs determined by measuring the intensities of the MTX peak at 1291 cm^{-1}. The standard deviations were obtained from independent measurements of three different cells

The experiments were extended to *in vivo* measurements on seven day old nude mouse involving Raman spectrometer and fluorescence microscopy (Figure 7). Raman spectra and fluorescence image were recorded from tumor side after injecting AuNPs-MTX conjugation under mouse skin before and after external GSH introduced. The decrease in SERRS intensities and recovery of fluorescence clearly show that the injected GSH triggered the release of MTX molecules from the surface AuNPs. The fingerprint peak of MTX at 1291 cm^{-1} was used to compare SERRS intensities before and after GSH treatment (inset Figure 7).

In the initial stage between 0-45 min, we could observe more rapid decrease in the SERRS measurement and a lag time in the NSET decay. This can be ascribed to a bond-breaking process that MTX would start to detach from AuNPs, if the difference in their distance dependence of the two methods is taken into account. The next decay profile between 45-120 min may be regarded as a typical diffusion-controlled process that can be fitted as a power law of m>0.5 in the equation of $C/C_o = Kt^m$, where C and C_o are the concentrations at the given times of t and zero, respectively.[27] The detached MTX spread out inside the cellular medium via either Fickcian diffusion or non-Fickcian relaxation/transport processes. Considering that the molecular weight and its estimated diffusion coefficient D value of 10^{-5}-10^{-4} cm^2/sec for MTX,[28] the diffusion length were estimated to be much longer than those of the dimension of AuNP aggregates inside either endosome or lysosome, which would be as short as 1 μm. A rather slow decay curve between 45-120 min may be due to an encapsulated state of MTX-AuNPs, which can affect and retard the diffusion process of free MTX. After 90 min, the NSET intensity became almost unchanged, which indicated that most MTX became alienated from AuNPs. In contrast to the NSET intensities, the significant SERRS intensities after a prolonged time of 60–120 min may be due to a trace amount of MTX on AuNPs in hot spots, which yields the signal in a non-quantitative way even on the decreased surface coverage density. Thus, fluorescent live-cell imaging techniques in comparison with SERRS yielded different decay rates in the estimation of drug release. Based on the average diameter of the AuNPs and a previous report on the value of R_o,[29] the distances for which the SERS and NSET would decrease by 50% would be 0.46 and 22 nm, respectively, assuming similar quenching behavior of MTX and cyanine-3B (λ_{max} = 570 nm) for ~15-nm AuNPs. It has to be mentioned that both a single cell microscopic and numerous cell (>10^3) fluorescence measurements using a microread-

er exhibited the similar decay profiles. In vivo images indicated that MTX release could be estimated by both Raman and fluorescence microscopy as shown in Fig. 8.

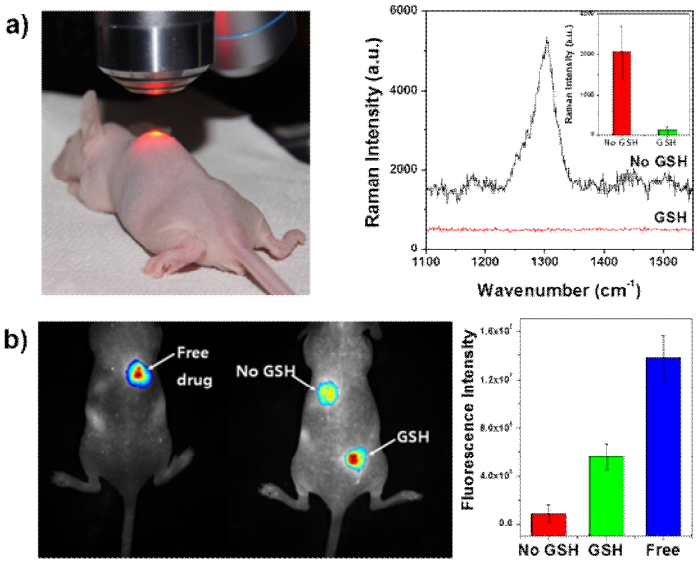

Fig. 7. (a) Photograph of thein vivo resonance Raman monitoring of GSH-triggered release (left). *In vivo* SERRS spectra of MTX and MTX-AuNPs in the presence and absence of GSH (right). The MTX peak at 1291 cm^{-1} almost disappeared after applying GSH. (b) *In vivo* fluorescence images of mice (left). Bar graph of the fluorescence intensities (right)

Discussion

Our results indicate that Raman and fluorescence spectroscopy can be employed to monitor the combinatory drug release from AuNPs.

References

1. Осипов О. А. Справочник по дипольным моментам. — Москва: Высш. шк., 1971. — 414 с.

2. Пентин Ю. А., Вилков Л. В. Физические методы исследования в химии. — М.: АСТ, 2003. — 683 с.

3. Enhancement of electro-optic properties in liquid crystal devices via titanium nanoparticle doping / Yong-Seok Ha, Hyung-Jun Kim, Hong-Gyu Park, and Dae-Shik Seo // “Homeotro-pic alignment of liquid crystals on a nano-

patterned polyimide surface using nanoimprint lithography," Soft Matter 7(12), 5610–5614 (2011).

ИССЛЕДОВАНИЕ ВЫСВОБОЖДЕНИЯ ПРОТИВОРАКОВЫХ ЛЕКАРСТВ ИЗ НАНОЧАСТИЦЫ МЕТОДОМ РАМАНОВСКОЙ СПЕКТРОСКОПИИ

Г. Эрдэнэ-Очир, Химический факультет,
Сунгсил университет, Сеул, Корея; Физический факультет,
Национальный университет Монголии
Улан-Батор, Монголия
E-mail: erdeneochir_g@num.edu.mn

С. У. Джоо, физический факультет,
Национальный университет Монголии
Улан-Батор, Монголия
E-mail: erdeneochir_g@num.edu.mn

Наночастицы золота лекарственно-сопряженная система AuNPs) были подготовлены самосборкой. Мы наблюдали за внутриклеточное высвобождение молекул лекарственного средства из AuNPs внутри одной клетки с использованием темного поля микроскопии-спектрометр комбинационного рассеяния в сочетании с помощью измерений в режиме реального времени без наклеек. были найдены иматиниба (КИМ) и топотекан (TOPO), которые образуют слабые ковалентные связи с AuNPs легко отделяться из-за внутриклеточного глутатиона (GSH), в то время как 4-карбоксильной бензолтиол используется в качестве сшивающего агента, остается на поверхности AuNPs.
Ключевые слова: поверхностный Гигантское комбинационное рассеяние, наночастицы золота, препарат де-ливрее, темнопольная микроскопии.